

General Disclaimer

One or more of the Following Statements may affect this Document

- This document has been reproduced from the best copy furnished by the organizational source. It is being released in the interest of making available as much information as possible.
- This document may contain data, which exceeds the sheet parameters. It was furnished in this condition by the organizational source and is the best copy available.
- This document may contain tone-on-tone or color graphs, charts and/or pictures, which have been reproduced in black and white.
- This document is paginated as submitted by the original source.
- Portions of this document are not fully legible due to the historical nature of some of the material. However, it is the best reproduction available from the original submission.

PRINCETON UNIVERSITY OBSERVATORY
Princeton, New Jersey 08544

(NASA-CR-176062) PHOTON-COUNTING IMAGE
SENSORS FOR THE ULTRAVIOLET Semiannual
Report (Princeton Univ. Observatory) 28 P
HC A03/MF A01 CSCI 14B

N85-31478

Unclas
G3/35 21884

Semi-Annual Report for NASA Grant
NSG-7618

Photon-Counting Image Sensors for the Ultraviolet

Covering the Period Ending July 31, 1985

Submitted to:

HEADQUARTERS
NATIONAL AERONAUTICS AND SPACE ADMINISTRATION
Washington, D.C. 20546

By:

Edward B. Jenkins
Edward B. Jenkins
Principal Investigator
Princeton University Observatory
Princeton, N. J. 08544
Tel: 609-452-3826



August 7, 1985

1. GENERAL SUMMARY

This grant supports three separate investigations on specific performance details of photon-counting, ultraviolet image sensors having 2-dimensional formats. In one study, we collaborated with Dr. G. Carruthers (U. S. Naval Research Laboratory [NRL]) to perform controlled experiments which compare the quantum efficiencies, *in pulse counting mode*, of CsI photocathodes deposited on (a) the front surface of a microchannel plate (MCP), (b) a solid surface in front of an MCP, and (c) an intensified CCD image sensor (ICCD) where a CCD is directly bombarded by accelerated photoelectrons. Tests indicated that the detection efficiency of the CsI-coated MCP at 1026 Å is lower by a factor of 2.5 than that of the MCP with a separate, opaque CsI photocathode, and the detection efficiency ratio increases substantially at longer wavelengths (ratio is 5 at 1216 Å and 20 at 1608 Å). Measurements of the efficiency of the ICCD arrangement were carried out last year, and a good portion of the data reduction is still in progress.

Another major investigation under this grant in the previous year was to determine whether or not there are any significant pore-interpore variations in the quantum efficiency of photocathodes deposited on MCP detectors. This study was carried out in collaboration with G. Timothy (Stanford Univ.) and R. Bybee (Ball Aerospace Systems Division [BASD]) who supplied a MAMA detector for a test run which was carried out last year under subcontract with BASD. A MAMA detector is one of the many types of image sensors which uses microchannel plates with photocathodes directly deposited on the front surface, or semi-transparent photocathodes on windows in front of the MCP.

In the initial tests carried out at BASD, we found periodic variations in response for the MAMA detector, with a spatial frequency equal to that of the pore spacing of the MCP. In addition, we found that the semi-transparent photocathode exhibited occasional, sharp drops in response (several tens of percent), as one

might expect from blemishes or scratches in the photocathode material. Figure 1 shows a plot of counting rate *vs* position, taken while the detector was scanned by a small spot of light. The defects can only be seen if the illumination spot size is as small as a few microns in diameter, which may explain why they have been overlooked in previous investigations. These findings may indicate that photocathodes created under normal image-tube manufacturing conditions may not be suitable for applications involving fine image detail. A report on the test setups at BASD and the results where the periodic variations were measured has been prepared by Mr. Bybee, and a copy of this report follows the next section.

Finally, Dr. Jenkins is reducing data from his recent successful flight of the Interstellar Medium Absorption Profile Spectrograph (IMAPS) which used an Intensified (electron-bombarded) CCD detector. These results, in conjunction with laboratory tests carried out at NRL (Dr. Carruthers's lab), will provide valuable data on the operating characteristics of these image sensors. Even without careful analysis, however, it is very clear that the ICCD performs very well.

The major thrust of our program for the current year is to continue the investigation of the microstructural variations in quantum efficiencies of MAMA detectors. In addition to measuring the amplitude of the variations, we will determine whether or not an ion barrier film on top of the MCP has a significant effect.

SMALL SPOT SCAN TESTS
RE-IMAGE GREEN LED
MCP = 2100V
PC = 2400V
THRESH = 0.6V
BIAS = 100/100V
STEP SIZE = 4.1 u/STEP

(A) RAW DATA PLOT
SUM OF 3 EA FINE
ANODES

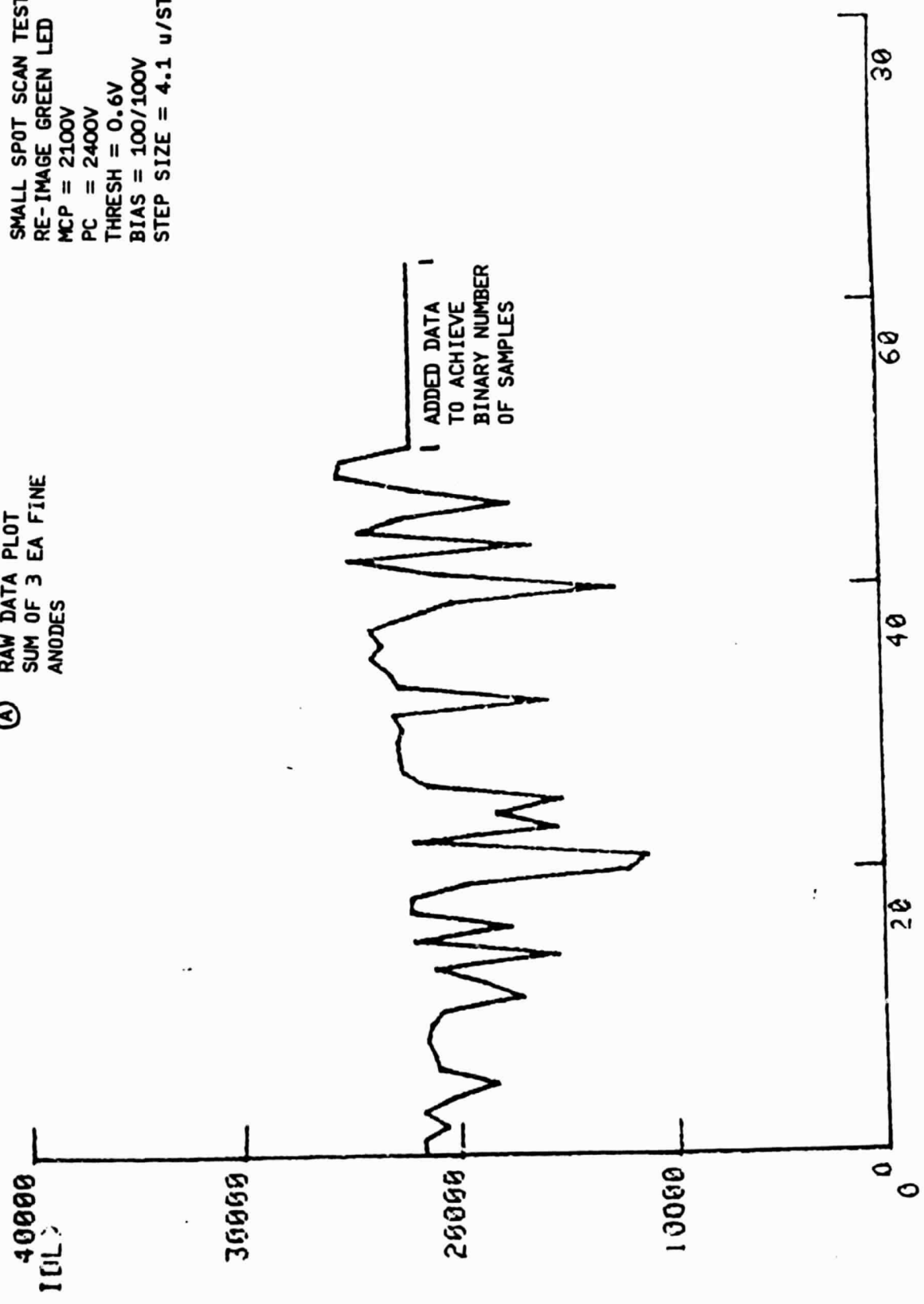


Figure 1.

2. RECENT ACTIVITIES AND PLANS

In early 1985, we purchased an all-reflecting microscope from Ealing Optics so that we could continue a more refined series of tests at Stanford University with newer detectors furnished by Dr. Timothy. At the same time, we shipped a precision x-y-z translation table driven by stepper motors from Princeton to Stanford (this device was available to this grant at no charge; it was purchased by an earlier NASA SR&T grant at Princeton and is now surplus equipment). In the spring and early summer of 1985, fixtures were made to support the MAMA detector and microscope objective, so that they could be moved by the table in precision translations with respect to the light source and pinhole.

During the week of August 19, Dr. Jenkins will travel to Stanford, and he and Dr. Timothy will perform the first run of testing with a relatively new style of MAMA detector. The properties of this detector are much better determined than those of earlier devices, and we expect the results of the new tests to build upon the earlier findings at BASD, but with more definitive conclusions.

3. BASD REPORT ON QUANTUM EFFICIENCY FLUCTUATIONS (excerpts)

(on pages which follow)

RESPONSE OF MICROCHANNEL PLATE DETECTORS TO SMALL
ILLUMINATION SPOT SIZES

| <u>TITLE</u> | <u>PAGE</u> |
|-----------------------------|-------------|
| 1.0 INTRODUCTION | 1 |
| 2.0 OBJECTIVE OF TEST | 1 |
| 3.0 APPROACH | 1 |
| 4.0 TEST SETUP | 4 |
| 5.0 PRE-SCAN TESTS | 5 |
| 6.0 RAW DATA | 6 |
| 7.0 PROCESSED DATA | 6 |
| 8.0 RESULTS | 6 |
| 9.0 ADDITIONAL DATA | 7 |

FIGURES

| | <u>TITLE</u> | <u>PAGE</u> |
|------------|--|-------------|
| FIGURE 1. | Sealed Detector Component Schematic | 8 |
| FIGURE 2. | Front View of Standard and Rectangular Actual Area Curved - Channel Microchannel Plates | 9 |
| FIGURE 3. | Front View of the (256x1024)-Pixel Coincidence Anode Array. The Central Active Area is Approximately 26 nm Across. | 10 |
| FIGURE 4. | Detail of Anode Structure | 11 |
| FIGURE 5. | Relative Orientation of Vertical Anodes to MCP Structure | 11 |
| FIGURE 6. | Electronics Block Diagram | 12 |
| FIGURE 7. | Example of Raw Data | 13 |
| FIGURE 8. | Optical Block Diagram | 14 |
| FIGURE 9. | Y15 Yaw Data | 15 |
| FIGURE 10. | Raw Minus Mean | 16 |
| FIGURE 11. | Cosine Bell | 17 |
| FIGURE 12. | B X C | 18 |
| FIGURE 13. | FFT of D | 19 |
| FIGURE 14. | Power Spectrum of E | 20 |

ATTACHMENTS

| | | |
|--------------|---|------------------------|
| ATTACHMENT A | Raw Data | 21 (not included here) |
| ATTACHMENT B | Variation of Response with Photocathode | see Fig 1. |

RESPONSE OF MICROCHANNEL PLATE DETECTORS TO SMALL ILLUMINATION SPOT SIZES

1. INTRODUCTION

This report describes a series of tests performed to determine the response of a microchannel plate detector to illumination spot sizes that are smaller than, or nearly the same size, as a single pore of the Micro-Channel Plate (MCP) itself. Test results obtained using a Multi-Anode Microchannel Plate Detector tube assembly indicate that the response of the MCP does indeed vary over spatial dimensions comparable to the spacing between pores in the MCP. The amplitude of the variation, for the specific geometry tested, was approximately 5.3% RMS.

2. OBJECTIVE OF TEST

There exists a number of applications for microchannel plate detectors in which it is possible that the optical spot size of the illumination will be nearly the same size as, or smaller than, the pore dimensions themselves (i.e. 8 to 25 microns). In order to predict the performance of the MCP under these conditions, it was deemed necessary to test an MCP under similar conditions using existing detector hardware. The objective of the test is to measure the variations in the photometric response of an MCP as a 2 to 5 micron diameter spot of light is scanned across the face of the MCP.

3. APPROACH

Initially, all tests were to be performed using an existing Ball Aerospace Systems Division IR&D (256x1024)-pixel image tube as the test device. This tube consisted of a bi-alkali photocathode in proximity focus with a curved-channel microchannel plate intensifier. The channel plate itself was read-out using an array of metal anodes to collect the output charge from the MCP. Each anode was connected to an electronics system capable of recording

(the occurrence of those MCP output charge pulses exceeding a present threshold of 60,000 electrons. Preliminary tests using this configuration demonstrated that a 5 micron image size at the MCP could not be obtained because of the limitations imposed by the proximity-focused photocathode. The sealed tube assembly was therefore modified to remove the photocathode (ultra-violet light would be used for subsequent tests) from the window and all future tests were to be performed with the illumination focused directly onto the microchannel plate itself.

A microscope objective and motor driven aperture assembly were used to re-image an illuminated 25 micron diameter aperture onto the microchannel plate. The image size reduction provided by the microscope objective was approximately a factor of twelve and thus a spot size somewhat smaller than the 12 micron pore diameter should have been obtained. The image of the aperture was scanned along an axis corresponding to the single top layer anodes in the anode array. Using this technique, only a single electronics channel need be used and any output count rate variations would be caused by MCP response variations rather than electronic circuit variations.

The scan across the MCP was performed in sixty-nine (69) steps of approximately four microns (4) each. At each step the number of counts (i.e. pulses that exceed 60,000 electrons) that occur on each of the ninety-six (96) anodes in the array were accumulated for an integration time of sixty (60) seconds. After each integration, a plot of the accumulated counts versus anode number was generated and a printout of the actual counts then listed below the plot.

Evaluation of the data consisted of plotting the accumulated output counts versus step number for the anode over which the image was focused. The plot was evaluated using an FFT to denote any output variation at the equivalent pore spacing frequency of 12 to 15 microns.

4. TEST SETUP

DETECTOR - The detector used to perform this series of tests was a (256x1024)-pixel MAMA assembly fabricated as part of the Ball Aerospace Systems Division internal research and development program. This tube was originally fabricated using a bi-alkali photocathode but was eventually reprocessed to remove the photocathode material from the window. This new configuration allowed the image to be focused directly onto the MCP using a "Pen-Ray" lamp as the UV source. As shown schematically in Figure 1, the two major components of the tube are the MCP and the anode array. Each of these are described below.

MCP - The MCP was a "curved-channel" microchannel plate fabricated by Galileo Electro-Optics. Although the outer diameter of the MCP was the standard 32mm, the active area as shown in Figure 2 was a (28x8)mm rectangle designed to match the shape of the anode array. The pores were 12 microns in diameter and located on 15 micron centers. The plate was operated in the "saturated mode" and provided a model gain of 5×10^5 and a FWHM of approximately 50%. The voltage applied to the MCP was typically 2200 volts.

Anode Array - The anode array used was a (256x1024)-pixel array designed for use in a coincidence array detector system. Figure 3 is a photograph of a similar array. For the purposes of this test however, the array was not operated in the coincidence mode. Rather, counts were recorded directly from each anode as illustrated in Figure 4. The vertically running anodes are approximately 10 microns wide and located on 25 micron centers. These anodes are thin-film aluminum and are connected directly to a charge-amplifier discriminator circuit as shown in the figure.

The anode array is operated in proximity focus to the rear face

of the MCP. The proximity gap is approximately 60 microns and is established by gold spacers between the MCP and the anode array. A voltage of 100 to 200 volts is used to minimize charge spreading between the MCP and the anode array. For all MCP response tests, the scan direction was run vertically along the vertical anodes. The orientation of the vertical anodes to the MCP pores is shown in Figure 5.

Electronics - An electronics block diagram is shown in Figure 6. As illustrated, each anode in the array is connected directly to a charge amplifier/discriminator. This circuit produces a 60 nanosecond logic pulse for each MCP charge event on that anode that exceeds a preset threshold (typically 60,000 electrons).

The number of logic pulses occurring in each channel in a preset period of time is recorded by accumulator circuits. These are periodically readout to a display computer for subsequent printing. An example of the data printout is shown in Figure 7.

Optical System - A block diagram of the optical test system is shown in Figure 8. As shown, the illuminated pinhole is imaged onto the MCP front face by a microscope objective assembly. The image of the 25 micron pinhole was reduced by the microscope objective by a factor of approximately twelve. Although it was not possible to measure spot size with the MCP detector, the performance of this optical set-up was verified using a similar detector window assembly and knife-edge detector to measure a visible light spot diameter. The illumination spot size was measured to be less than 5 microns wide at the 50% points. This size spot (or smaller) is compatible with the measurement goals.

The pinhole aperture plate is mounted on a stepper-motor driven

translation assembly capable of steps as small as 2.5 microns. Because of the image size reduction, however, step sizes of 50.8 microns were used to produce an illumination movement of approximately 4.5 microns on the MCP. Thus, each of the 69 steps recorded was separated by 4.5 microns on the MCP.

5.0 PRE-SCAN TESTS

Three tests were performed in order to verify proper test system operation prior to scan tests. These tests include:

- o Focus - To optimize focus, the aperture image was centered over fine anode Y15 and the focus distance varied until the response on adjacent anodes was minimized. The distance was then centered between the fore and aft extremes where spreading did occur. While it is recognized that this is not, in itself, verification of 5um or better focus, this test provided the best focus possible. The previously performed knife-edge test demonstrated that 5um focus is achieved under similar circumstances.
- o Image Size Reduction - Image size reduction was measured by scanning the aperture image between top layer fine anodes whose center to center spacing is known to be 51 um. The average number of 50.8 micron aperture plate steps required to move the image 51 um was approximately 11.5. The image step size was thus determined to be approximately 4.5 microns.
- o Microchannel Plate Linearity - With the image focused near the operating area of the MCP, an ND filter was inserted in the optical path and the approximate attenuation noted. The operating count rate used during the test was approximately 20 C/S/ANODE.

6. RAW DATA

All data obtained were produced in the form of plots of anode count rate versus anode number. These data are shown in Attachment A for all integrations taken during the scan.

7. PROCESSED DATA

The processing of data included the following steps:

- A. Plot of intensity versus step number for anode "Y₁₅". Results are shown in Figure 9.
- B. Plot of (Intensity-mean value) versus step number for anode "Y₁₅". This step removes the D.C. component for subsequent FFT. Results are shown in Figure 10.
- C. Generate Cosine Bell used to remove high-frequency components caused by limited sample space. The plot of this curve is shown in Figure 11.
- D. Multiply Cosine Bell (C) times plot (B) to produce data used as input to the FFT program. The results are shown in Figure 12.
- E. Perform FFT using IDL program residing in BASD VAX computer. Results are shown in Figure 13.
- F. Generate "Power Spectrum" of E using the IDL program. Results are shown in Figure 14.

G. RESULTS

The power spectrum shown in Figure 14 shows a strong peak in the spectrum at a frequency of 23 cycles in the scan of 310 microns. This frequency appears to correspond to the pore spacing of 12 to 15 microns. The amplitude of this variation can be found by using:

$$(\text{RMS Variation})^2 = A \times F$$

where

A = peak amplitude

F = frequency interval = 1/34.5

For the logarithmic plot shown, only the peak at the 23rd sample is of significance.

$$(\text{Variation})^2 = \frac{1.4 \times 10^5}{35} = 4058$$

$$\text{RMS Variation} = \sqrt{4058} \approx 64$$

$$\text{Variation (\%)} = \frac{64}{1211} = 5.3\%$$

9.0 ADDITIONAL DATA

Attachment B shows the results of the intensity plot taken for the tube using a proximity focused photocathode. Of interest here are the rapid variations in output count rate for small (4.5 um) steps. While the cause of this variation has not been identified, it is suspected that it is the result of structure in the photocathode material.

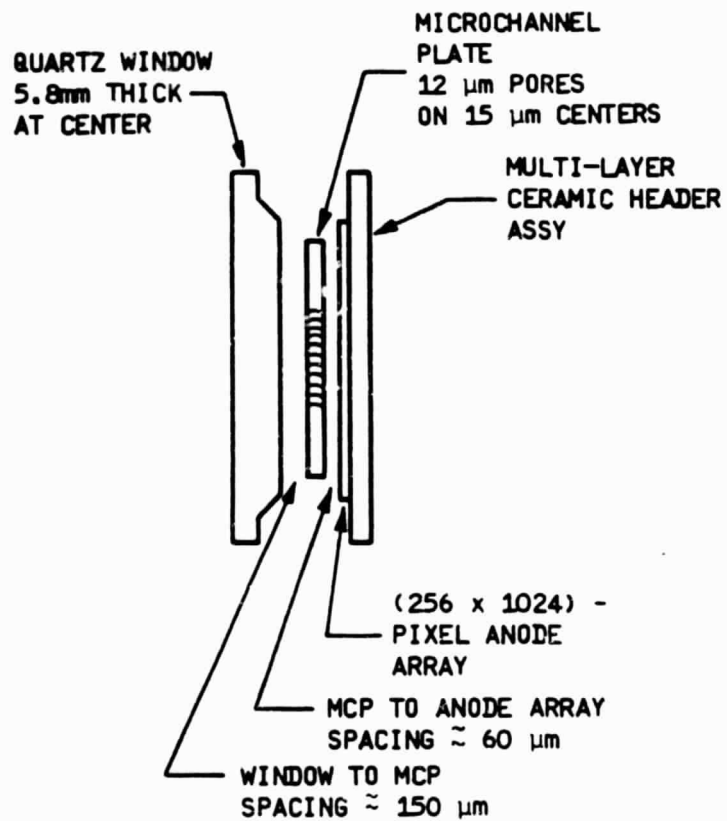


FIGURE 1. Sealed Detector Component Schematic

A/N 5290

ORIGINAL PAGE IS
OF POOR QUALITY



FIGURE 2. Front View of Standard and Rectangular Actual Area Curved -
Channel Microchannel Plates

ORIGINAL PAGE IS
OF POOR QUALITY

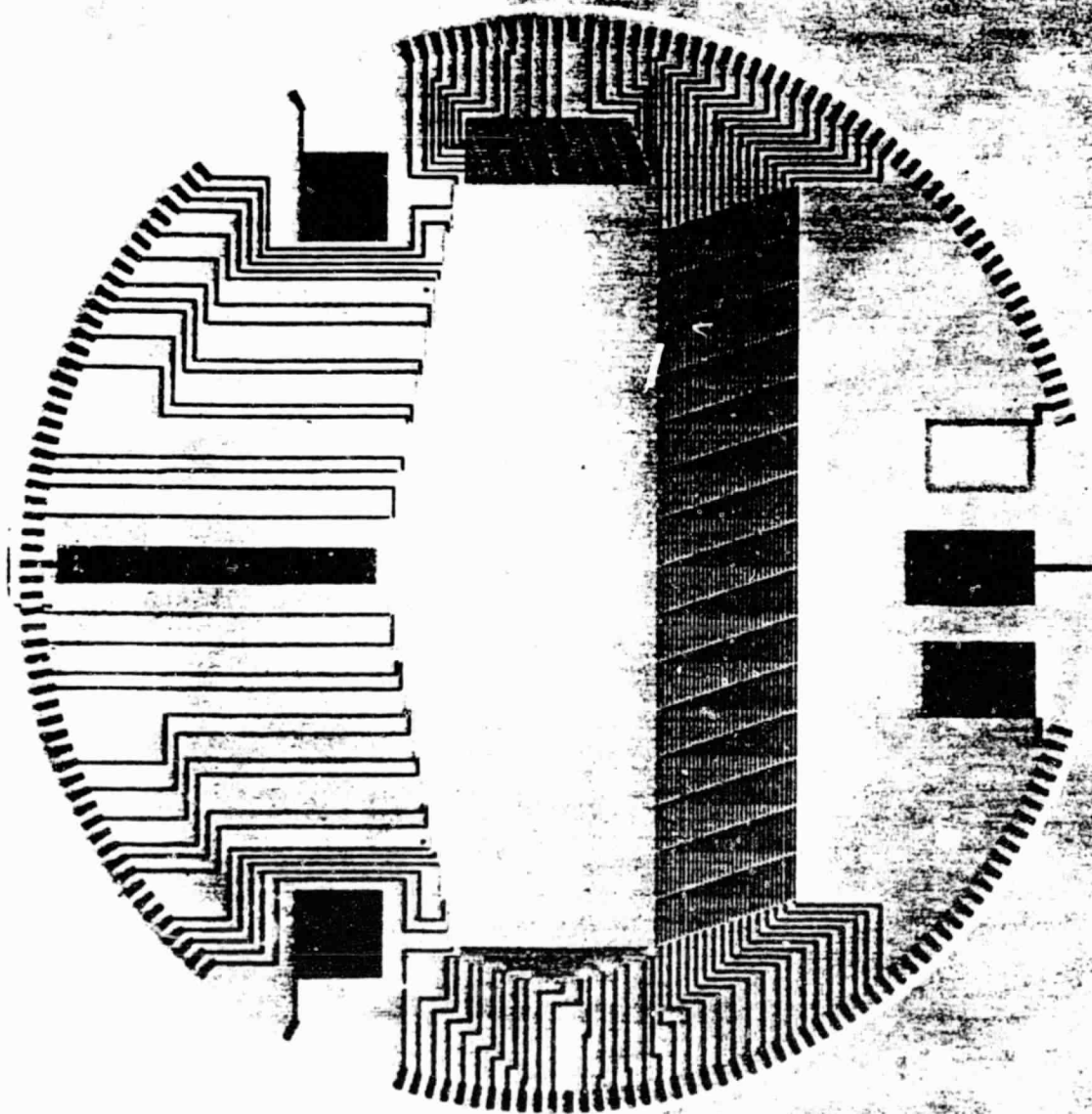


FIGURE 3. Front View of the (256x1024)-Pixel Coincidence Anode Array. The Central Active Area is Approximately 26 mm Across.

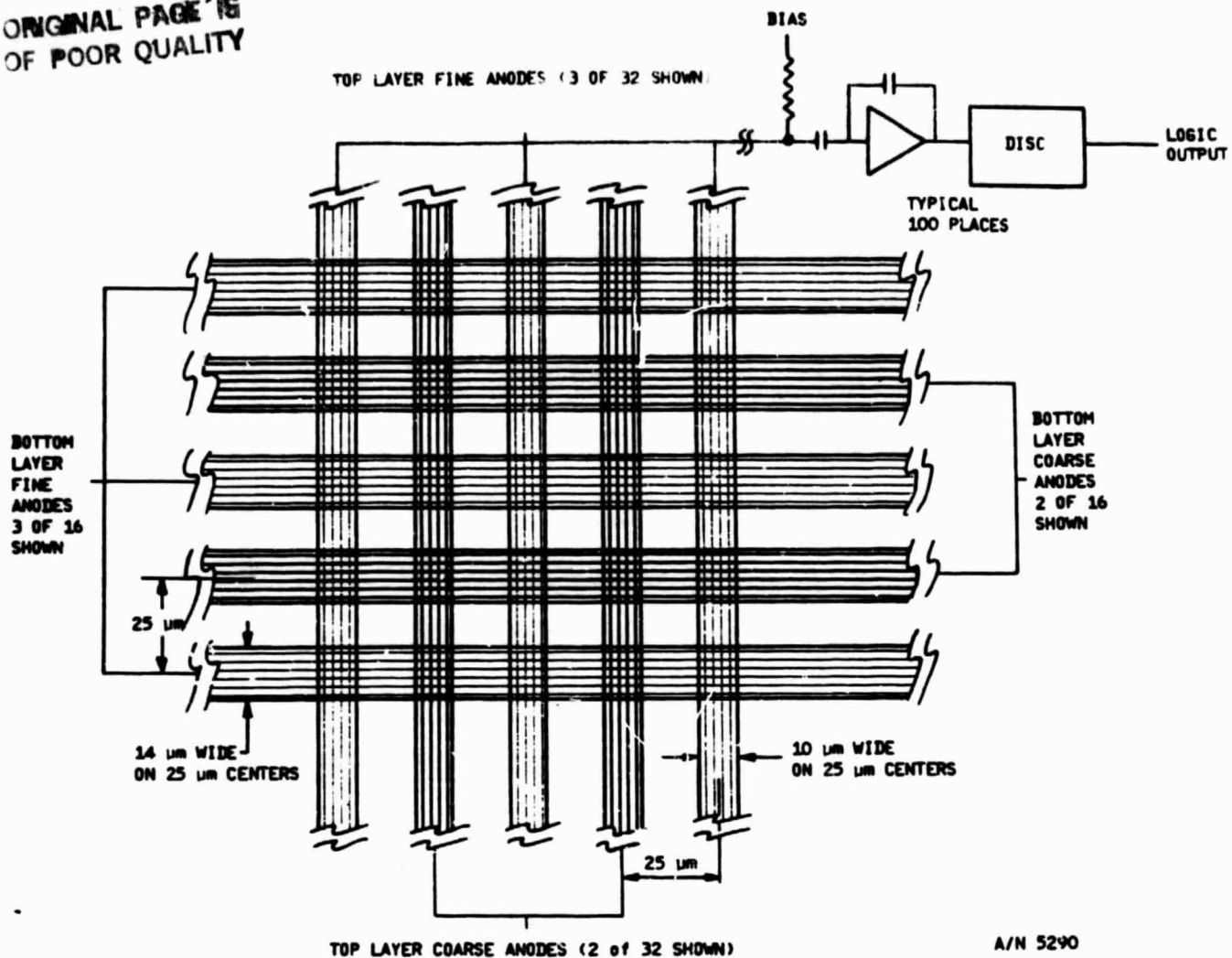


FIGURE 4. Detail of Anode Structure

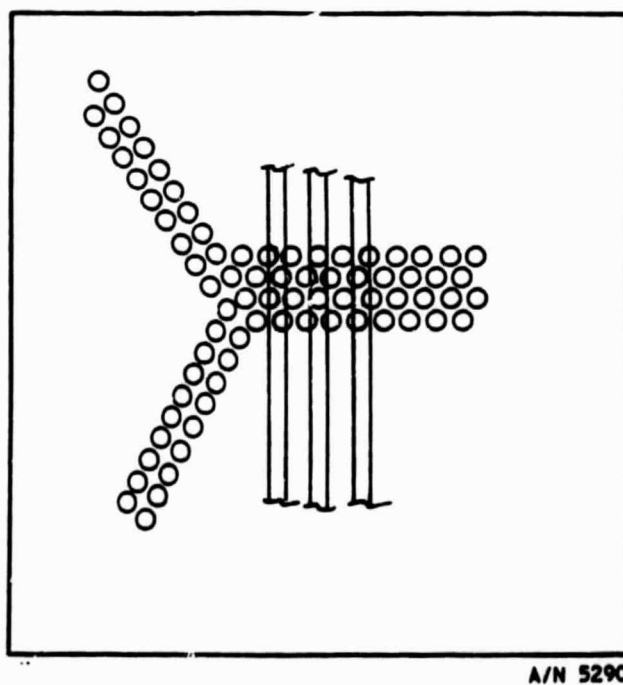
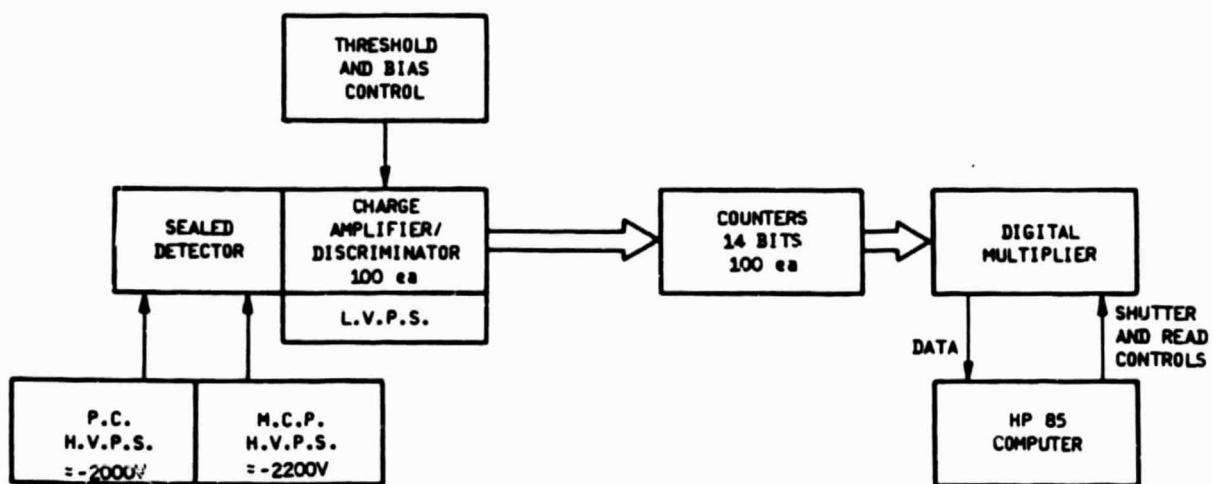


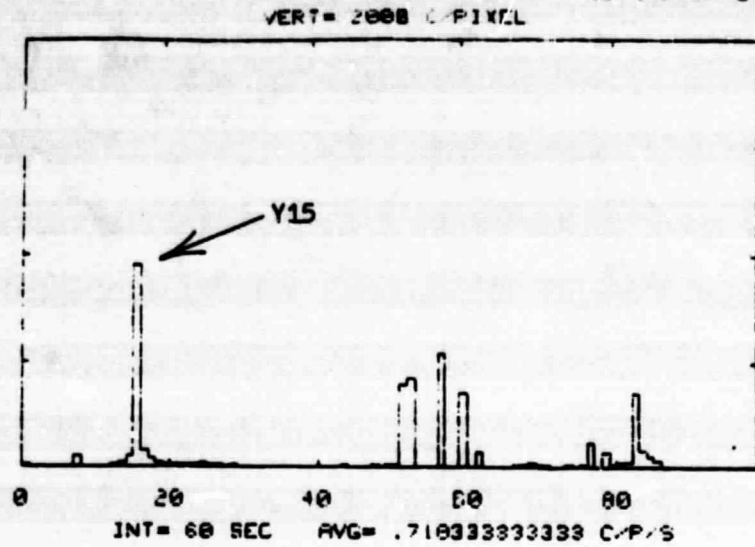
FIGURE 5. Relative Orientation of Vertical Anodes to MCP Structure



A/N 5290

FIGURE 6. Electronics Block Diagram

ORIGINAL PAGE IS
OF POOR QUALITY



INT = 60 AVE = 42.62
MULT = 1

| | | | | | |
|----|-----|-----|-----|----|-----|
| 0 | 10 | 2 | 6 | 4 | 0 |
| 5 | 3 | 7 | 52 | 4 | 6 |
| 10 | 3 | 8 | 14 | 25 | 51 |
| 15 | 948 | 86 | 41 | 27 | 11 |
| 20 | 11 | 12 | 14 | 13 | 19 |
| 25 | 10 | 13 | 8 | 10 | 7 |
| 30 | 8 | 5 | 0 | 3 | 4 |
| 35 | 5 | 1 | 3 | 4 | 8 |
| 40 | 7 | 6 | 4 | 13 | 9 |
| 45 | 4 | 7 | 10 | 8 | 10 |
| 50 | 11 | 396 | 420 | 6 | 6 |
| 55 | 3 | 533 | 0 | 0 | 352 |
| 60 | 4 | 72 | 0 | 1 | 0 |
| 65 | 0 | 13 | 10 | 19 | 10 |
| 70 | 11 | 5 | 5 | 9 | 4 |
| 75 | 9 | 120 | 0 | 75 | 18 |
| 80 | 19 | 22 | 353 | 79 | 49 |
| 85 | 30 | 7 | 0 | 5 | 3 |
| 90 | 5 | 3 | 2 | 5 | 4 |
| 95 | 4 | 4 | 7 | 0 | 0 |

FIGURE 7

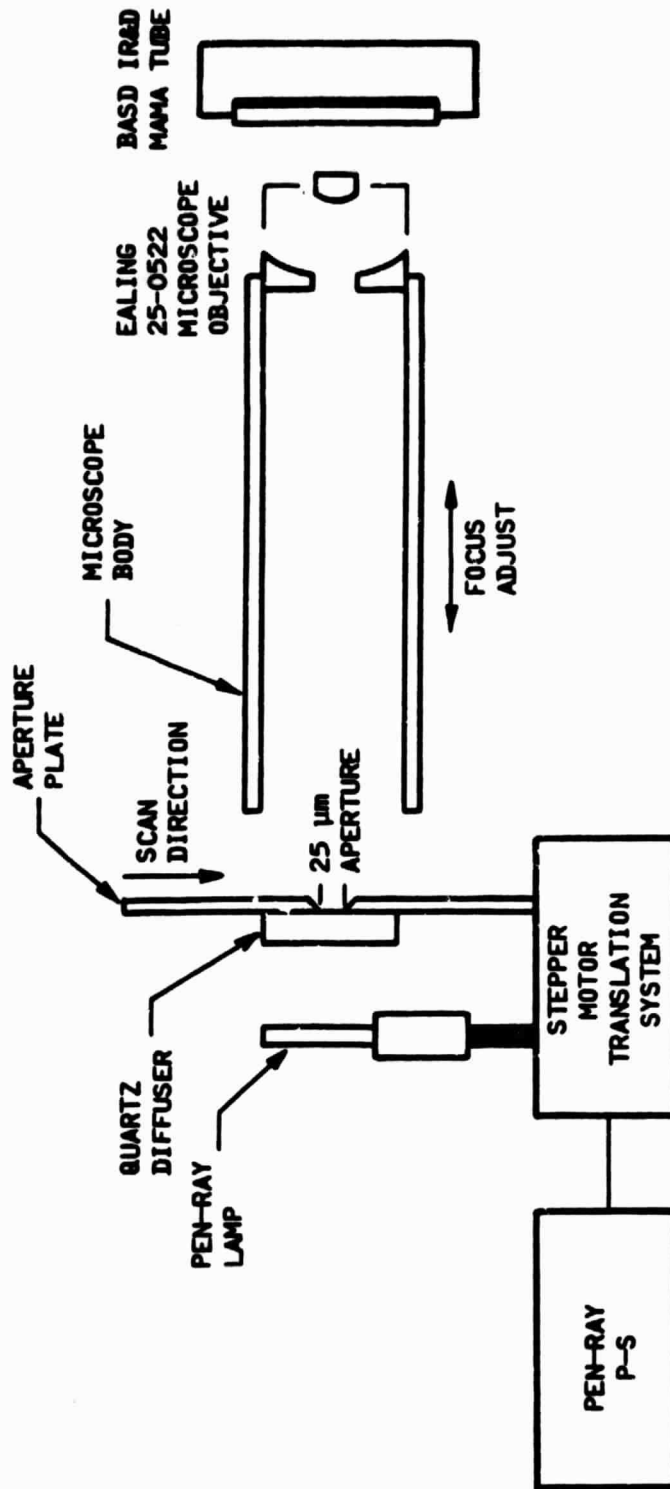


FIGURE 8. Optical Block Diagram

A/N 5290

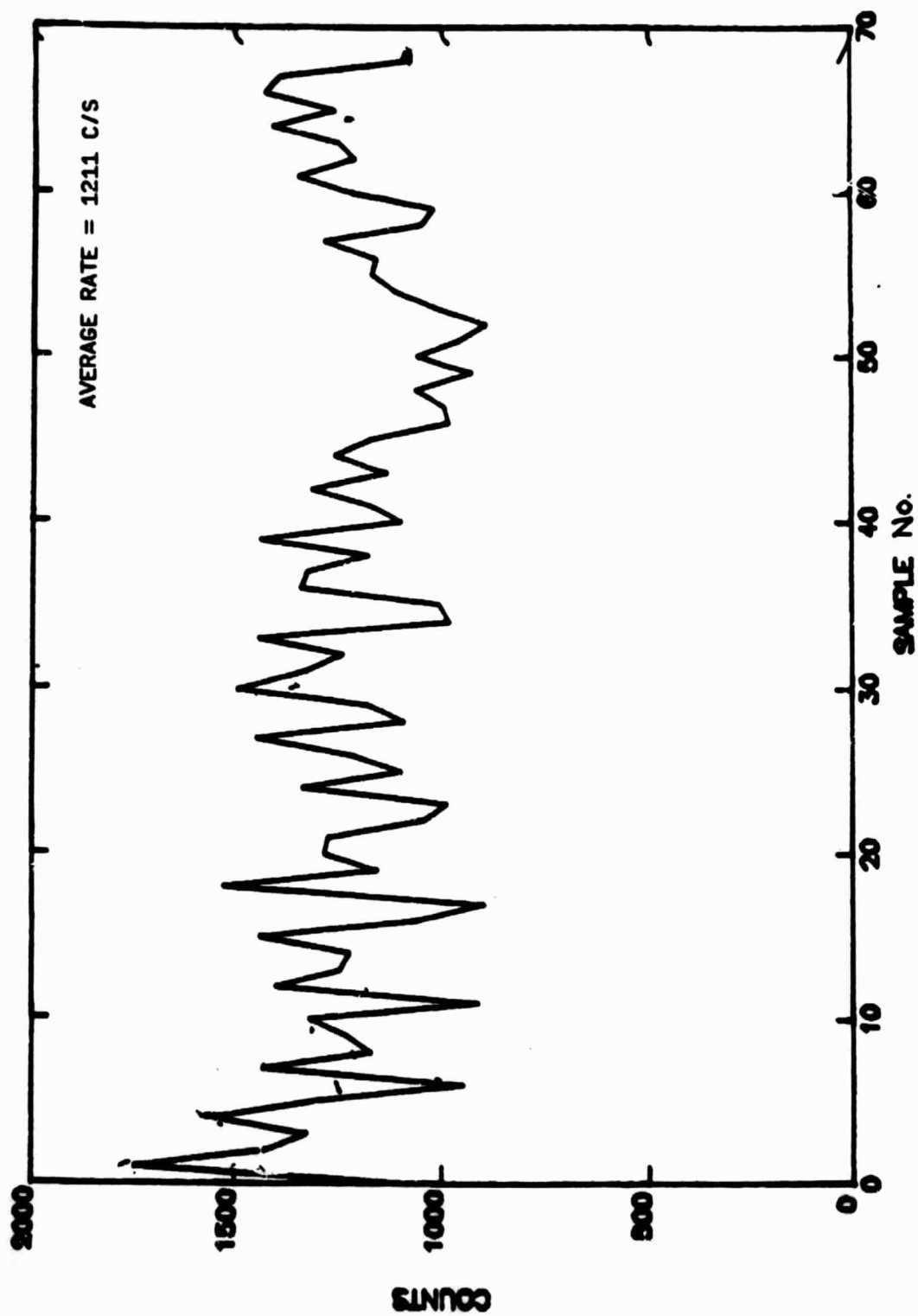


FIGURE 9. Y15 RAW DATA

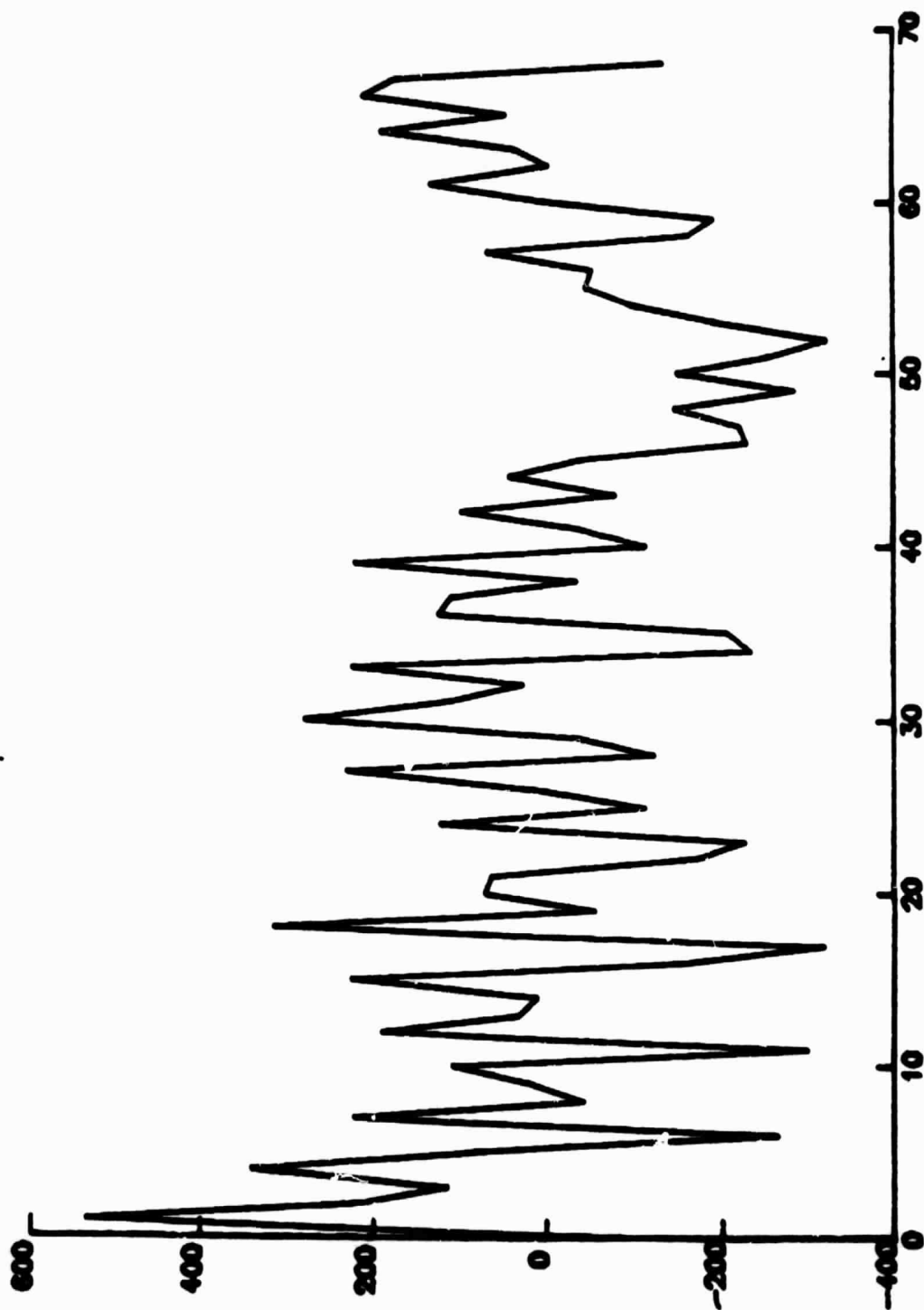


FIGURE 10. Raw Minus Mean

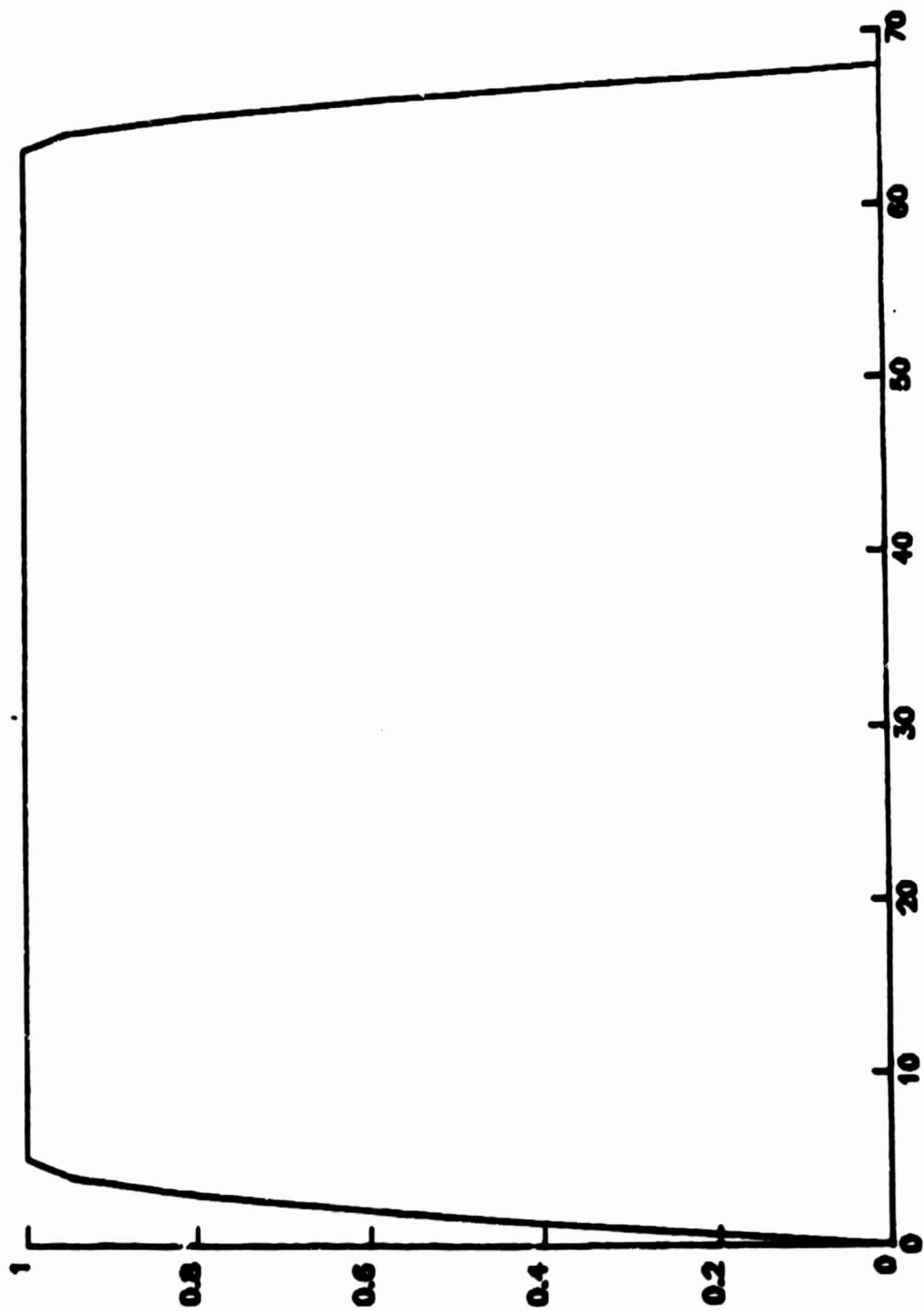


FIGURE 11. Cosine Bell

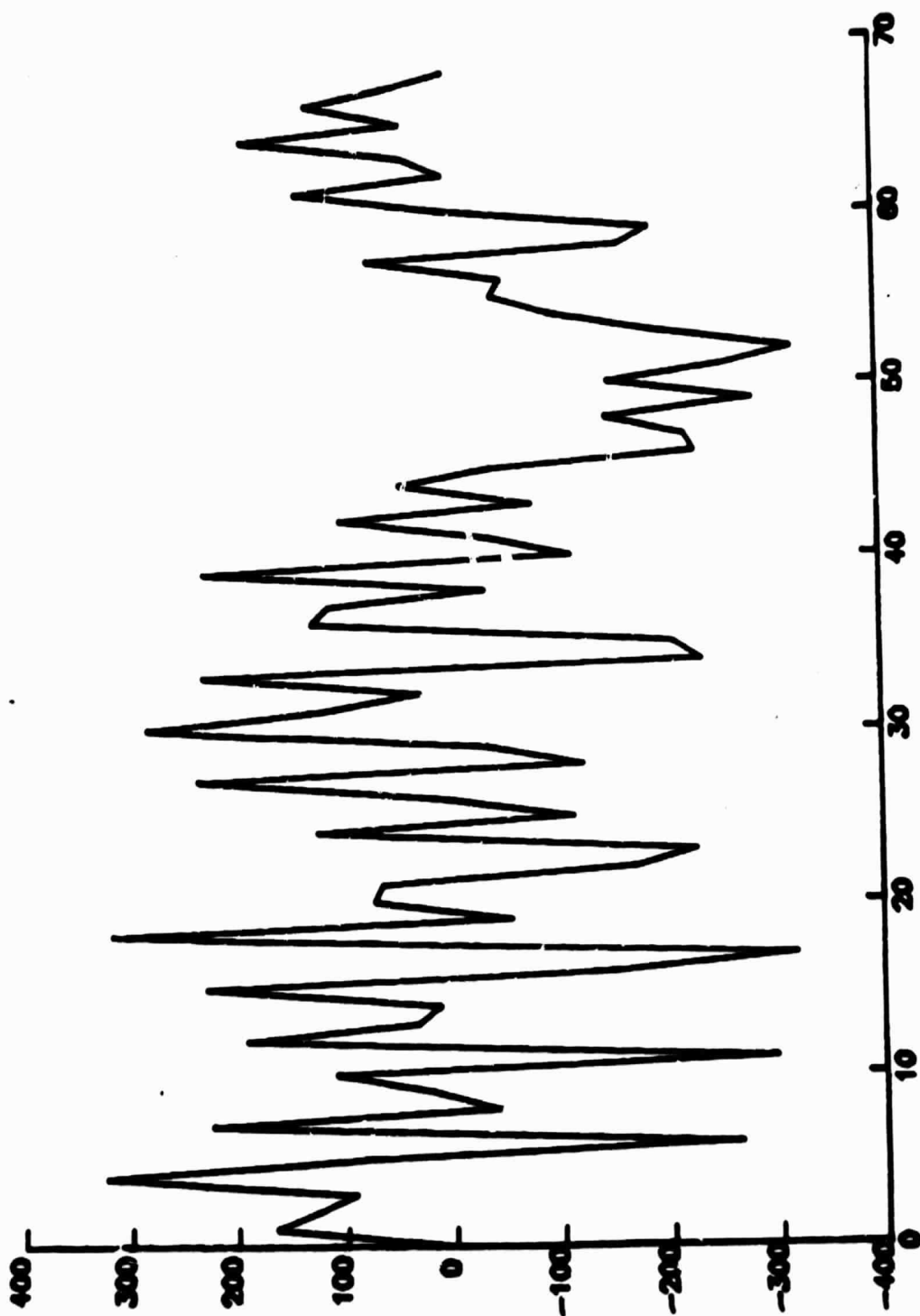


FIGURE 12. B X C

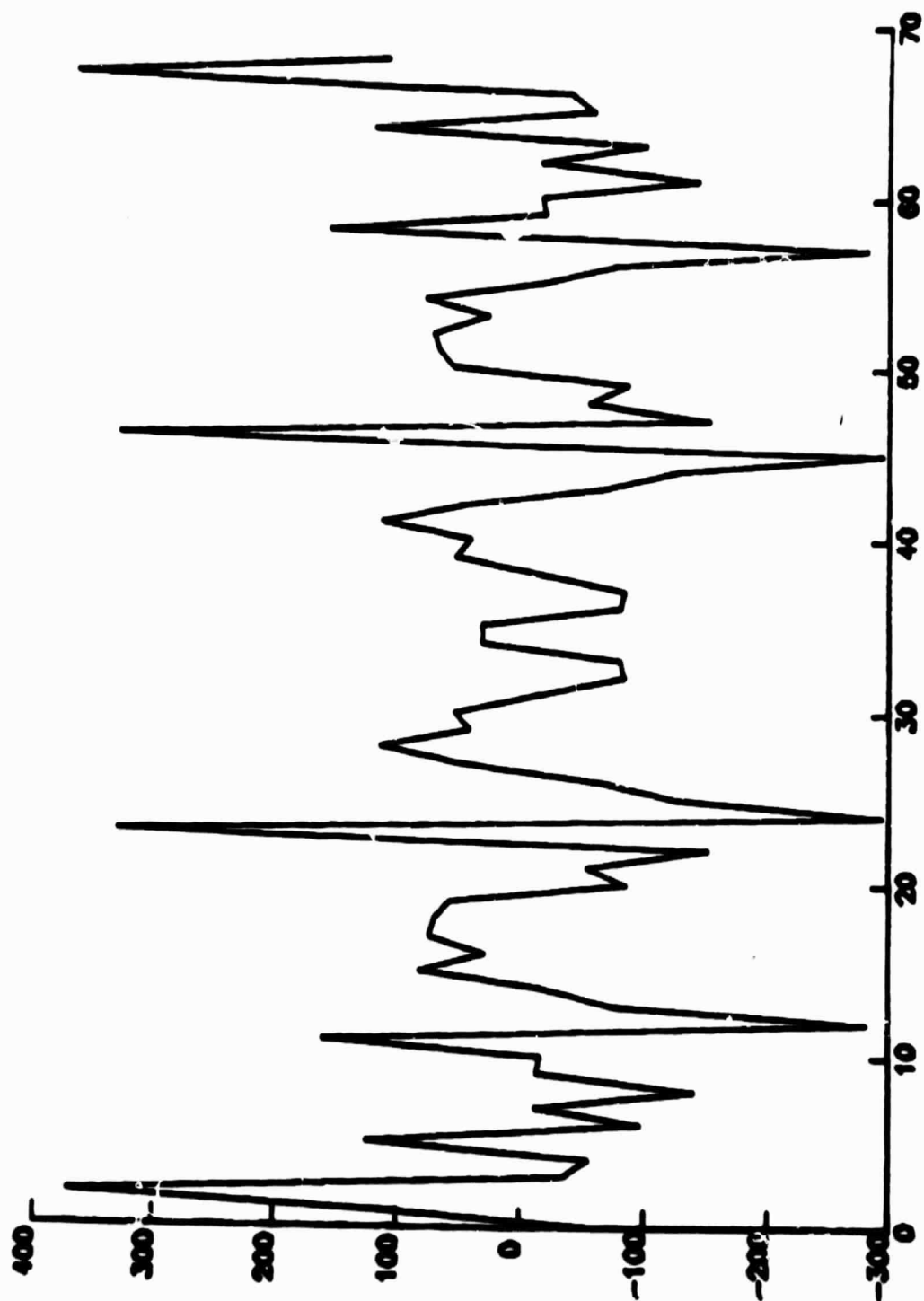


FIGURE 13. FFT of D

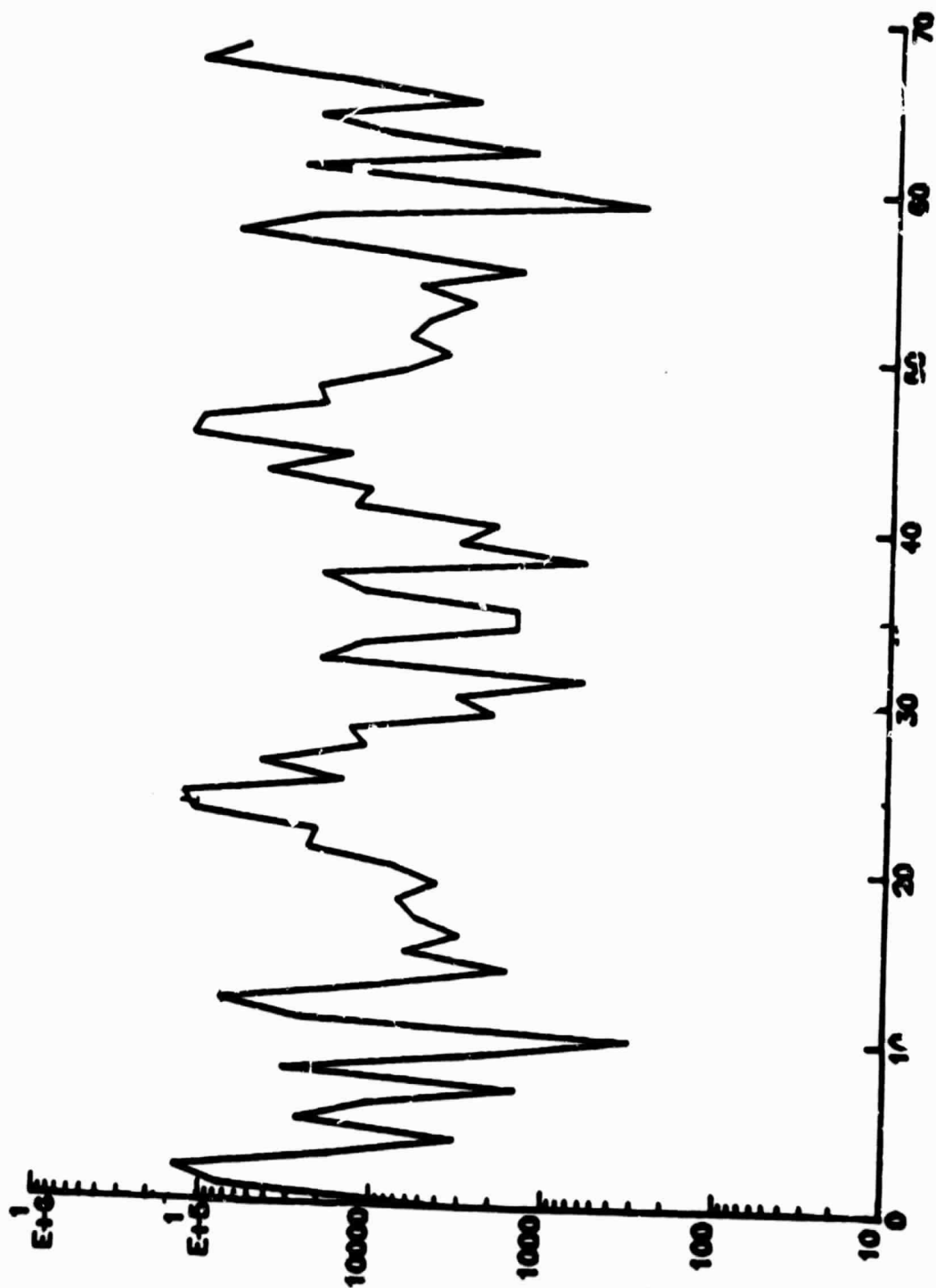


FIGURE 14. Power Spectrum of E